

# Using Re-W $\sigma$ -phase first-principles results in the Bragg-Williams approximation to calculate finite-temperature thermodynamic properties

Suzana G. Fries

ACCESS e.V., RWTH-Aachen, D-52072 Aachen, Germany

Bo Sundman

Department of Materials Science and Engineering, Royal Institute of Technology, S-10044 Stockholm, Sweden

(Received 14 February 2002; published 24 June 2002)

First-principles (FP) calculations of total energies for 32 different configurations of Re-W  $\sigma$  phase were used to fit a compound energy formalism (CEF) Hamiltonian that was used in phenomenological Calphad method calculations to model finite-temperatures thermodynamic properties. A comparison with Connolly-Williams method–cluster variation method (CWM-CVM) calculations indicates that the first-principles CEF (FP-CEF) describes temperature-dependent site occupancies as well as the CWM-CVM approximation within the temperature range of interest for applications. This result seems to indicate that the Bragg-Williams approximation (BWA) is sufficient to describe the Re-W  $\sigma$  phase. A complete Re-W phase diagram is calculated using the FP-CEF Hamiltonian for the  $\sigma$  phase. Differences between the phase diagrams, and single phase properties calculated both with, and without, the first-principles results are striking. It is expected that using the FP-CEF  $\sigma$ -phase description that takes into account the first-principles energetics will yield more reliable extrapolations into higher-order system.

DOI: 10.1103/PhysRevB.66.012203

PACS number(s): 81.30.Bx, 64.60.Cn, 64.90.+b, 82.60.Lf

## I. INTRODUCTION

The compound energy formalism<sup>1,2</sup> (CEF) is commonly used within the Calphad method<sup>3</sup> to model complex multi-component systems with: phases that have interstitials; intermetallic phases with wide homogeneity ranges; or phases with order/disorder transformations. The first  $\sigma$  phase described thermodynamically with CEF was in the Cr-Fe system<sup>4</sup> and current databases have thermodynamic descriptions of  $\sigma$  phases with 5–15 components, e.g., Ref. 5. Because there are very few experimental data on site occupancies of  $\sigma$  phases it is very useful to calculate them from first principles (FP). But a previous paper<sup>6</sup> describing FP calculations for the Fe-Cr  $\sigma$  phase failed to reproduce experimental site occupancies.

Recently, Berne *et al.*<sup>7</sup> published a FP study of the  $\sigma$  phase in Re-W. They presented total-energy calculations for 32 different configurations of Re and W on the 30 sites in the  $\sigma$ -phase unit cell. The Connolly-Williams method<sup>8</sup> (CWM) was used to obtain a cluster expansion Hamiltonian for calculation of site occupancies as functions of temperature and composition, using cluster variation method (CVM).<sup>9</sup> We fit our CEF coefficients to the Berne *et al.*<sup>7</sup> total-energy results, and model the  $\sigma$  phase in a phenomenological Calphad calculation;<sup>10</sup> the FP-CEF results are then compared with Berne *et al.*<sup>7</sup> CWM-CVM results. The CEF is a generalized Bragg-Williams approximation, which implies random distributions of components within each crystallographic site; i.e., short-range order is ignored.

## II. THE CEF

The general Gibbs energy expression is

$$G_m = G_m^{srf} - T S_m^{conf} + G_m^{xs}. \quad (1)$$

The surface of reference for the model is the sum of Gibbs energies of all configurations with atom  $i$  on each sublattice  $s$  weighted by the site fractions  $y_i^{(s)}$ . The  $\sigma$  phase has five sublattices with different numbers of sites and coordinations and can be described as  $(\text{Re,W})_2(\text{Re,W})_4(\text{Re,W})_8(\text{Re,W})_8(\text{Re,W})_8$ , sites 1–5, respectively. This gives  $2^5 = 32$  ordered configurations. Thus, the surface of reference becomes

$$G^{srf} = p_{ijklm} {}^o G_{ijklm},$$

$$p_{ijklm} = y_i^{(1)} y_j^{(2)} y_k^{(3)} y_l^{(4)} y_m^{(5)}. \quad (2)$$

These compound energies,  ${}^o G_{ijklm}$ , are exactly the same FP energies calculated in the paper by Berne *et al.*<sup>7</sup>

The only additional term necessary to calculate the Gibbs energy at any temperature is the entropy of mixing that is assumed to be ideal in CEF

$$S^{conf} = -R \sum_s a^{(s)} \sum_{i=\text{Re,W}} y_i^{(s)} \ln(y_i^{(s)}), \quad (3)$$

where  $a^{(s)}$  is the number of sites on sublattice  $s$ . This means one can directly calculate the properties of the  $\sigma$  phase in CEF from the FP results (FP-CEF). No pair- or higher-order effective cluster interaction parameters<sup>8</sup> are needed to obtain temperature-dependent properties.

## III. RESULTS AND COMPARISON

Direct comparison between the FC-CEF and CWM-CVM (Ref. 7) calculations of site fractions as functions of composition and temperature are shown in Figs. 1(a) and 1(b). Note that the diagram at 1500 K, Fig. 1(a), is almost identi-

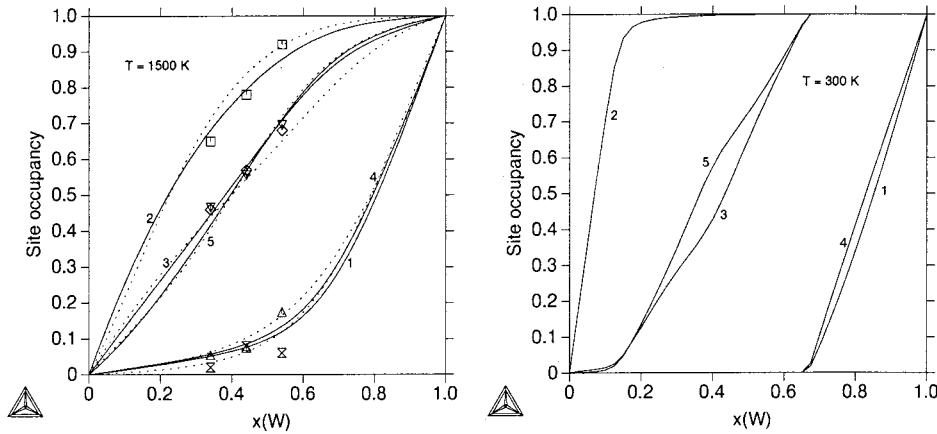


FIG. 1. Site occupancies at two different temperatures. (a) FP-CEF calculated site occupancies at 1500 K. (b) FP-CEF calculated site occupancies at 300 K.

(a) FP-CEF calculated site occupancies at 1500 K

(b) FP-CEF calculated site occupancies at 300 K

cal to the CWM-CVM results (their Fig. 5, here plotted as dashed lines).

At temperatures below 1000 K the results of the two model calculations differ, in Fig. 1(b) a calculation at 300 K is shown that can be compared with Fig. 4 in Berne *et al.* Site occupancies of sublattices preferred by Re and W are almost the same as those predicted by Berne *et al.*,<sup>7</sup> but the fractions in sublattices with mixed composition are quite different from the CWM-CVM results. The  $\sigma$  phase is not stable at these temperatures, so experimental verification is problematic.

In Fig. 2 site occupancies and heat capacity are plotted as functions of temperature. Above 1000 K there is practically no difference between Fig. 2(a) and the analogous CWM-CVM diagram, Fig. 7 in Ref. 7. It is interesting to note that the rapid change in site occupancies below 500 K corresponds to a peak in the heat capacity Fig. 2(b).

IV. CONCLUSIONS AND PERSPECTIVES

Site occupancy diagrams are critical for describing the properties of the  $\sigma$  phase. The FP-CEF yields as good an approximation of the temperature and composition depen-

dencies of  $\sigma$ -phase site occupancies as the CWM-CVM calculations; at least for temperatures well above 500 K, which is the range of practical interest. This suggests that short-range order, which was ignored in the FP-CEF calculation, may not be essential for modeling topologically closed-packed (TCP) phases such as  $\sigma$ .

There is an assessed Re-W description using CEF in the thermodynamic database referenced above (old). It is now interesting to compare some properties of the  $\sigma$  phase from this database with the FC-CEF description (present). In Fig. 3(a) the excess heat capacity for the FC-CEF description is compared with CEF one, which was modeled with Kopp-Neumann's rule and thus has zero excess heat capacity.

The CEF description was obtained by fitting a simplified  $\sigma$  phase model that assumed the same mixing on three sublattices, only Re on one, and only W on another sublattice; i.e.,  $(\text{Re})_8(\text{W})_4(\text{Re,W})_{18}$ . With this simplification there are only two terms in the  $G^{srf}$  term and these can be fitted to the scarce experimental data. In Fig. 3(b) the enthalpy of the FP-CEF-fitted  $\sigma$  phase is compared to the CEF fitted; reference states are  $\sigma$  Re and  $\sigma$  W. In the stable range for  $\sigma$

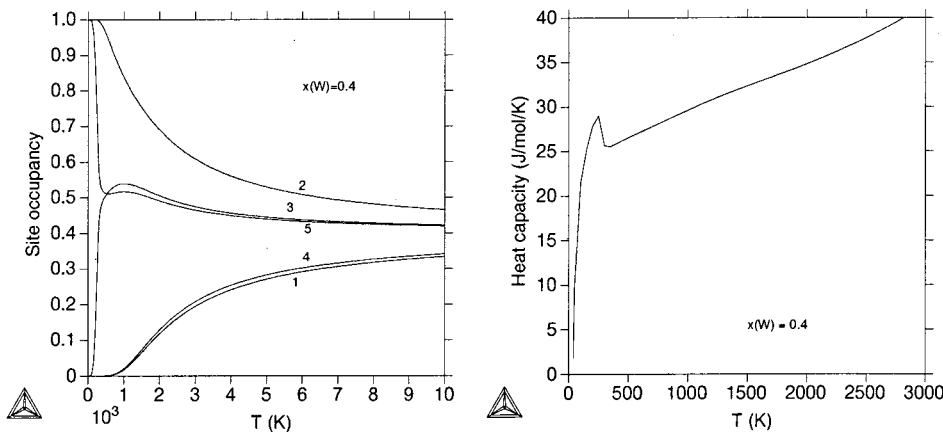


FIG. 2. Site occupancies and heat capacity as functions of temperature. (a) FP-CEF calculated site occupancies at  $x(w)=0.4$ . (b) FP-CEF calculated heat capacity at  $x(w)=0.4$ .

(a) FP-CEF calculated site occupancies at  $x(w)=0.4$

(b) FP-CEF calculated heat capacity at  $x(w)=0.4$

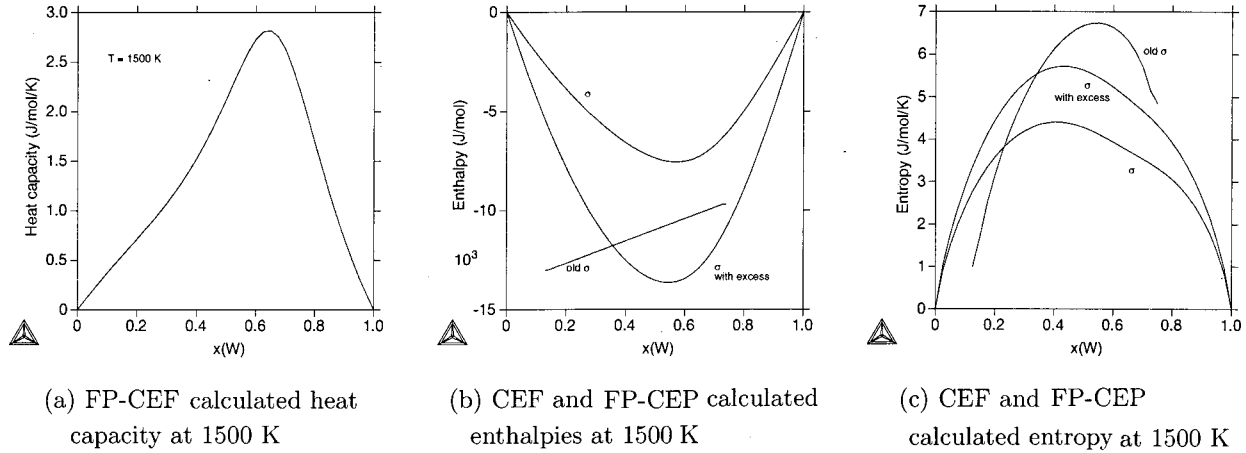


FIG. 3. Comparisons between  $\sigma$  for old (CEF) and present (FP-CEF) models. (a) FP-CEF calculated heat capacity at 1500 K. (b) CEF and FP-CEF calculated enthalpies at 1500 K. (c) CEF and FP-CEF calculated entropy at 1500 K.

phase, the enthalpies are not very different, but CEF model did not extend to the pure elements and gave much lower enthalpy at high Re content. Such differences can be very important when extrapolating the data for a binary assessment to multicomponent systems.

The FP-CEF description of the  $\sigma$  phase was fitted into the CEF old assessment without changing the descriptions of any other phases. The additional parameters needed are values for the difference between Gibbs energies for the pure elements in the  $\sigma$  phase relative to other phases, and a value of  $H_{Re}^{\sigma}(T=0\text{ K}) - H_{Re}^{hcp}(T=0\text{ K}) = 16\,300\text{ J/mol}$   $H_{W}^{\sigma}(T=0\text{ K}) - H_{W}^{bcc}(T=0\text{ K}) = 20\,200\text{ J/mol}$  taken from.<sup>12</sup> Entropy values for the pure elements in the  $\sigma$  phase were fitted subject to the constraint that the  $\sigma$  phase does not become stable at pure element compositions. The final Gibbs energies are

$$\begin{aligned} {}^{\circ}G_{Re}^{\sigma} - {}^{\circ}G_{Re}^{hcp} &= 16\,300 - 2.62T, \\ {}^{\circ}G_{W}^{\sigma} - {}^{\circ}G_{W}^{bcc} &= 20\,200 - 4.55T. \end{aligned} \quad (4)$$

Additionally a contribution depending only on composition and temperature is used

$$G^{ex} = x_{Re}x_{W}L_{Re,W}, \quad (5)$$

where  $x_i$  is the mole fraction of  $i$  and  $L_{Re,W} = -24\,700 - 5.4T$ . In Fig. 3(b) the FP-CEF enthalpy calculated with and without this excess contribution is shown. A small adjustment of one parameter in the  $\chi$  phase was needed to describe the temperature of the invariant equilibria at 2400 K.

In Fig. 3(c) the entropy as function of composition at 1500 K is shown calculated using the CEF (old) and the FP-CEF (present)  $\sigma$  models, with and without the contribution of Eq. (5).

The old phase diagram is shown in Fig. 4(a) and the present one in Fig. 4(b). The largest difference occurs at the low temperature where the  $\sigma$  phase is stable to lower temperatures and for higher W contents. This is a direct effect of the better FP-based energetics on the site occupancy. Without the FP results, there was no constraint on the eutectoid composition. There is an Calphad assessment in the literature<sup>13</sup> that gives a phase diagram very similar to the one calculated

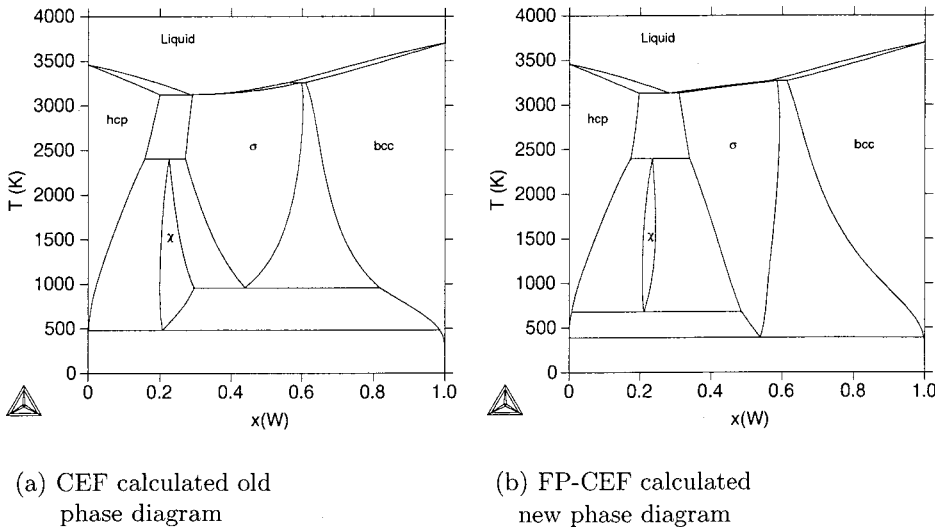


FIG. 4. Different  $\sigma$  phases in Re-W. (a) CEF calculated old phase diagram. (b) FP-CEF calculated present phase diagram.

here using the FP energetics. However, the enthalpy of the  $\sigma$  phase is not better than in the CEF  $\sigma$  model presented here.

The contribution from the Eq. (2) and Eq. (3) only depends on configuration and the excess term, Eq. (5), added to the phase description in order to fit the phase diagram, is only depending on composition. The CEF Hamiltonian used in this work can be written as

$$G_m = H_m^{confFP}(y) - TS_m^{confBW}(y) + G_m^{conf-indep}(x, T). \quad (6)$$

This kind of separation of contributions is already used with some success in Calphad assessments.<sup>2,11</sup>

Further comparisons with calculations of the thermodynamic properties using the CWM CVM and FP-CEF will be very interesting. It is expected that this description of the Re-W  $\sigma$  phase, which is available in Ref. 14, yields better extrapolations into higher-order systems where the precipitation of  $\sigma$  phases are critical, for example, in the development of new high-temperature Ni-based superalloys. More FP calculation of formation energies for relaxed atomic configura-

tions with different structures of TCP phases, and more generally for the so-called Hume-Rothery phases, in the binary subsystems of Ag-Al-Cu-Co-Cr-Fe-Hf-Nb-Ni-Re-Ta-Ti-W-Zn, are very helpful. A similar treatment of Re-Ta system is in progress.

#### ACKNOWLEDGMENTS

The authors gratefully acknowledge Marcel Sluiter for providing the original data for the formation energies and for the CVM results dashed in Fig. 1. The authors thank Benjamin Burton for his patient critical reading of the manuscript and for his suggestions bridging interdisciplinary jargon and give special thanks to Nathalie Dupin who promptly provided the experimental data she collected for the system. This work is partially supported by DFG (Deutsche Forschungsgemeinschaft) within the Collaborative Research Center 370 "Integrated Modeling of Materials" and by the Deutsche Zentrum für Luft-und Raumfahrt e.V. (DLR), Grant No. 50WM 0043 and by a grant from the Swedish Strategic Research Foundation (SSF).

<sup>1</sup>I. Ansara, T. G. Chart, A. Fernandez Guillermet, F. H. Hayes, U. R. Kattner, D. G. Pettifor, N. Saunders, and K. Zeng, CALPHAD: Comput. Coupling Phase Diagrams Thermochem. **21**, 171 (1997).

<sup>2</sup>I. Ansara, B. Burton, Q. Chen, M. Hillert, A. Fernandez-Guillermet, S. G. Fries, H. L. Lukas, H.-J. Seifert, and W. Alan Oates, CALPHAD: Comput. Coupling Phase Diagrams Thermochem. **24**, 19 (2000).

<sup>3</sup>N. Saunders and A. P. Miodownik, in *Calphad*, edited by R. W. Cahn, Pergamon Materials series Vol. 1 (Elsevier, Oxford, 1998).

<sup>4</sup>J.-O. Andersson and B. Sundman, CALPHAD: Comput. Coupling Phase Diagrams Thermochem. **11**, 83 (1987).

<sup>5</sup>N. Dupin and B. Sundman, Scand. J. Metall. **30**, 184 (2001).

<sup>6</sup>M. Sluiter, K. Esfarjani, and Y. Kawazoe, Phys. Rev. Lett. **75**,

3142 (1995).

<sup>7</sup>C. Berne, M. Sluiter, Y. Kawazoe, T. Hansen, and A. Pasturel, Phys. Rev. B **64**, 144103 (2001).

<sup>8</sup>J. W. D. Connolly and A. R. Williams, Phys. Rev. B **27**, 5169 (1983).

<sup>9</sup>R. Kikuchi, Phys. Rev. **81**, 998 (1951).

<sup>10</sup>B. P. Burton, N. Dupin, S. G. Fries, G. Grimvall, A. F. Guillermet, P. Miodownik, W. A. Oates, and V. Vinograd, Z. Metallkd. **92**, 514 (2001).

<sup>11</sup>B. Sundman, S. G. Fries, and W. A. Oates, CALPHAD: Comput. Coupling Phase Diagrams Thermochem. **22**, 355 (1998).

<sup>12</sup>C. Berne, Dr thesis, Intitut Nacional Polytechnique de Grenoble, France, 2000.

<sup>13</sup>Z. Liu and Y. A. Chang, JALCOM **299**, 153 (2000).

<sup>14</sup><http://www.sgte.org>